RESEARCH MEMORANDUM

A STUDY OF THE AERODYNAMIC LOADS ON SWEPTBACK WINGS AT TRANSONIC SPEEDS

By Claude V. Williams and Richard E. Kuhn

Langley Aeronautical Laboratory
Langley Field, Va.

NATIONAL ADVISORY COMMITTEE
FOR AERONAUTICS

WASHINGTON

June 25, 1953

NATIONAL ADVISORY COMMITTEE FOR AERONAUTICS

RESEARCH MEMORANDUM

A STUDY OF THE AERODYNAMIC LOADS ON SWEPTBACK WINGS AT TRANSONIC SPEEDS

By Claude V. Williams and Richard E. Kuhn

SUMMARY

A study of the aerodynamic loads on sweptback wings at transonic speeds has indicated that, for thick wings, the spanwise center of pressure moves inward, whereas for thin wings, the center of pressure moves outward with increase in Mach number; and increases in the sweep angle of a thin wing cause the spanwise center of pressure to move progressively outboard. Washing out a thin swept wing to approximate the effects of aeroelastic twisting shifted the spanwise center of pressure inboard and at a Mach number of 1.00, this shift was primarily due to the loss in load over the trailing edges of the outboard portions of the span. An investigation of the effects of sideslip on the loads over a swept-wing—curved-body combination indicated that increase in sideslip angle increased the relative load over the forward wing such that even though the spanwise center of pressure of the wing remained constant, the root bending-moment coefficients were increased.

INTRODUCTION

The recent development of transonic wind tunnels has enabled experimental investigations to be performed which have provided information at transonic speeds of considerable interest in the field of aerodynamic loads. Also high-subsonic-speed wind-tunnel measurements of the aerodynamic loads resulting from asymmetrical flight attitudes have recently been made. These several investigations are of current interest since, at the present time, the available theoretical methods for calculation of the various loading parameters used in the structural design of aircraft wings are seriously hampered by the regions of separated and mixed flows which exist about configurations operating at transonic speeds, and thus these parameters must be evaluated experimentally. The purpose of this report is to present the results of a study of the available experimental information concerning the aerodynamic loads on sweptback wings at transonic speeds. This study was concerned primarily with an

evaluation of the effects of thickness ratio, aeroelastic twisting, and sideslip. In order to simplify the presentation and to expedite publication, descriptions of the various model configurations and detailed data from the several investigations are not presented herein but will be found in the various reports for each investigation.

RESULTS AND DISCUSSION

Thickness-Ratio Effects

At transonic speeds, wing-section-thickness ratio appears to be one of the most important geometrical parameters. For example, a recent high-subsonic-speed wind-tunnel investigation has indicated that variation of Reynolds number from 2,000,000 to approximately 4,500,000 (based on the wing mean aerodynamic chord) caused rather large changes in the spanwise load distribution of a representative thick swept wing (ref. 1). However, a comparison of the data obtained from transonic-speed investigations of a typical thin swept wing has shown that variation of Reynolds number from 2,000,000 to approximately 6,000,000 produced little or no effect on the spanwise load distribution on the wing (refs. 2 and 3).

The effects of thickness ratio on the spanwise or lateral center-of-pressure variations with Mach number M are shown in figure 1. Spanwise center-of-pressure data are of interest in that, for a given design load, the spanwise location of the center of pressure directly determines the values of the wing root bending moments. In figure 1, as in the following figures, the spanwise center-of-pressure location y_{cp} is expressed in terms of the semispan of the wing outside the body $(b/2)_e$.

The dashed-line curve in figure 1 shows the typical inward movement of the spanwise center of pressure with increase in Mach number that has been observed for thick swept wings. These particular data were obtained from flight measurements on a current fighter-type airplane having a wing sweep angle Λ of 35° and approximately 9-percent-thick streamwise airfoil sections (ref. 4). The solid-line curve indicates the typical outward shift of the spanwise center of pressure with increase in Mach number that has been noted for thin swept wings. These data were interpolated from transonic wind-tunnel measurements of a 6-percent-thick, 45° sweptback wing (ref. 2). The curves are presented for a normal-force coefficient of 0.4 which is within the moderate normal-force-coefficient range where the wing tips are relatively free from stall effects, and, therefore, the variations shown are indicative of the conditions when the spanwise center of pressure is at, or near, its most outboard position. A rather limited analysis of the available transonic-speed, sweptback-wing data has been made, and this analysis indicated that

[redacted]

the transition from thick-wing to thin-wing characteristics takes place at thickness ratios on the order of 6 or 7 percent.

Because of certain aerodynamic advantages, primarily the reduction of the wing drag at transonic and supersonic speeds, most future airplanes will have thin wings. In view of the opposing trends shown by the curves in figure 1, it is apparent that care should be used when extrapolating center-of-pressure data obtained from current thick-wing configurations for use in the structural design of future thin-wing airplanes to avoid a serious underestimation of the values of the root bending moments of the thin wing.

Since thin wings will be utilized in future aircraft designs, a more detailed discussion of the center-of-pressure characteristics of the typical thin swept wing should be of interest. This analysis will be based on the data of figure 2 which shows the spanwise center-of-pressure variation with Mach number at several angles of attack α for the thin-wing—curved-body configuration shown in the figure. The data presented were obtained from reference 2 except for the variation at an angle of attack of 10° which was obtained from unpublished data. The wing had 45° sweepback of the quarter-chord line, aspect ratio of 4, taper ratio of 0.6, and NACA 65A006 streamwise airfoil sections.

From the curves of figure 2, it may be seen that in the transonic-speed range, the spanwise center of pressure was relatively outboard at angles of attack of 4° to 10° which at a Mach number of 1.0 corresponds to normal-force coefficients on the order of 0.35 to 0.75. However, the most outboard location occurred at an angle of attack of 8° and a Mach number of 1.0. This most outboard location of the spanwise center of pressure generally represents the critical conditions for maximum root bending moments.

Pitch-up occurs at angles of attack somewhat higher than 8° for this configuration and an analysis of pitch-up characteristics has shown that, if pitch-up occurs, the maximum design loads can be exceeded by a considerable amount. For the pitch-up case, the maximum loads would occur at some angle of attack higher than 8° for this configuration, and would depend upon the particular dynamic characteristics of the specific airplane in question.

Further, in the design of a wing, the combination of bending and twisting loads at the critical loading condition would be considered. However, since these twisting effects are usually small in relation to the effects of the bending loads, defining the critical root bending conditions by considering only the bending loads gives a good approximation of the critical loading conditions.

[redacted]

Another factor to consider when determining the critical loading condition is the effect of various wing auxiliary devices such as a fence. At subsonic speeds, fences on a swept wing delay the onset of tip stall, which would result in a more outboard location of the spanwise centers of pressure for the higher angles of attack. However, in the transonic-speed range, wing fences generally become ineffective, and, therefore, the critical loading conditions would be unaffected by a wing fence.

The data shown in figure 3 indicate some of the effects on the variations of the spanwise center-of-pressure location with Mach number that result from increases in the angle of sweep of a thin wing. These data were obtained from an investigation made in the Langley high-speed 7- by 10-foot tunnel. All of the wings shown in the figure had an aspect ratio of 3, taper ratio of 0.14, and NACA 65A003 streamwise airfoil sections. These data are in the unstalled lift-coefficient range where the most outboard centers of pressure occur and show that the location of the spanwise center of pressure is relatively constant at subsonic speeds, moves outboard in the transonic-speed range, and then moves inboard again at supersonic Mach numbers. Also, in the transonic-speed range, increase in sweep angle progressively moved the spanwise center-of-pressure locations outboard and raised the Mach number at which the maximum outboard locations of the center of pressure occurred. Although the center-of-pressure movements shown may appear to be small, it should be pointed out that at the 40-percent-semispan station, for example, a center-of-pressure shift of 3 percent of the semispan changes the value of the root bending moment by some $7\frac{1}{2}$ percent of its value. Also in figure 3, it may be noted that the 37° sweptback wing had a plan form similar to a delta wing, and, therefore, the center-of-pressure characteristics shown give some idea of the characteristics of delta wings at transonic speeds.

Aeroelastic Twisting

Recently, a geometrically twisted, sweptback wing has been investigated in the Langley 8-foot transonic tunnel. This wing had a plan form that was identical to the plan form of the wing for which the critical bending moment conditions were determined from the data of figure 2. A comparison of these two wings gives some idea of the changes in loading that result from aeroelastic twisting due to the deflection of a sweptback wing under load.

A plan-form view of the model is shown in figure 4. Also, in figure 4 is shown the spanwise variation of the local section angles of attack when the body center line was at an angle of attack of 0°. As seen from the plot, the wing was twisted about the quarter-chord line such that the tip was washed out approximately $4\frac{1}{2}$°. The twist of this

wing is considered to be a typical variation, and does not represent the twist of any particular type of wing structural system. In the following figures, the twisted wing will be compared with the similar untwisted wing shown in figure 2. In the subsequent discussion, this untwisted wing will be referred to as the plane wing. Both the plane and twisted wings were investigated on the body shown in figure 4 instead of the curved body shown in figure 2. These wings are to be compared at the critical bending conditions of Mach number of 1.0 and angle of attack of 8° determined for the plane wing. Also, in order to provide an idea of the twist effects at subsonic speeds, a parallel comparison at a typical subsonic Mach number of 0.80 is presented.

Figure 5 presents the comparison of the spanwise distributions of the section normal-loading coefficient for the subsonic and critical transonic-speed conditions. The section normal-loading coefficient is defined as the section normal-force coefficient c_n multiplied by the ratio of the local section chord c to the average wing chord $\bar{c}$. These data are compared at wing normal-force coefficients C_{N_W} equivalent to an angle of attack of 8° for the plane wing; that is, 0.46 for the subsonic case and 0.53 for the transonic-speed case. For the twisted wing these normal-force coefficients correspond to angles of attack of approximately $10\frac{3}{4}^\circ$ and 10°, respectively. It may be seen from the figure that, although the general shapes of the distributions at the two Mach numbers are dissimilar, the general effects of twist in both cases is, as would be expected, a reduction in the load over the outboard regions of the span and an increase in load over the inboard sections of the wing.

Figure 6 presents a comparison of the distributions of the pressure coefficient P for the plane and twisted wings at the subsonic Mach number of 0.80, and wing normal-force coefficient of 0.46. One of the first things to be noted in this figure is that the pressure-coefficient distributions over the lower surfaces of the wings are essentially the same. By referring to figure 5, the changes in loading may be correlated with the variations of the upper-surface pressure-coefficient distributions. The pressure-coefficient distributions shown in figure 6 indicate that the increase in load for the twisted wing was located over the forward portion of the chord for the most inboard station. At the center sections of the span, the load over most of the chord was reduced, and at the tip, the distributions were virtually unchanged.

For the transonic-speed, critical-bending case, the pressure-coefficient distributions shown in figure 7 indicate, as for the subsonic speed case, that the major differences in loading between the plane and twisted wings were concentrated on the upper surfaces of the wings. Over the inboard regions, the difference in loading extended over much of the chord length, but at the outboard sections, the distributions

[redacted]

show that the main reductions in loading were restricted to the trailing edges of the wing tip region. From practical considerations, this change in loading would have considerable effects on any control surfaces located in this region of the span.

Figures 8 and 9 present a summary of the center-of-pressure characteristics of the plane and twisted wings at Mach numbers of 0.80 and 1.00, respectively. The plan-view sketch in figure 8 shows the convention used to define the locations of the spanwise and chordwise centers of pressure. The chordwise center of pressure x_{cp} defines the point of intersection with the average wing chord $\bar{c}$ of a line which is parallel to the wing quarter-chord line and upon which the wing center of pressure is located. The chordwise center of pressure is measured parallel to the body center line and is expressed in terms of the average wing chord.

In figure 8, it may be seen that the spanwise center of pressure of the twisted wing was inboard of that for the plane wing throughout the wing-normal-force-coefficient range of this investigation. The data presented correspond to angles of attack from 4° to 20°. At the higher normal-force coefficients, the tips of the twisted wing have not stalled to as great a degree as the tips of the plane wing, and, therefore, the curves tend to converge.

The chordwise center-of-pressure curves in figure 8 indicate that at subsonic speeds twisting the wing had little or no effect on the location of the chordwise center of pressure.

Figure 9 shows that at a Mach number of 1.00 in the low and moderate wing-normal-force-coefficient range, the spanwise center of pressure of the twisted wing, as at subsonic speeds, was relatively inboard of that for the plane wing. Also, it may be seen that the tip stall trend at the higher normal-force coefficients pointed out for the subsonic case has progressed to a degree where the curves are the same.

At this point, it will be of interest to point out the relationship of the chordwise center of pressure to the characteristics of the spanwise center of pressure. It has been shown that twisting the wing moved the spanwise center of pressure inboard. However, for a conventional wing which usually has the elastic axis located in the 35- to 40-percent-chord region, the forward location of the chordwise center of pressure ahead of the elastic axis, such as is shown in figure 9, would tend to increase the local section angles of attack, and therefore move the spanwise center of pressure outboard. In general, however, these effects are small and, for any specific case, would depend upon the structural rigidity of the particular wing in question. The chordwise center-of-pressure curves in figure 9 show at a Mach number of 1.00 that geometric twisting had little or no effect on the location of the chordwise center of pressure. However, it may be seen for both wings that the twisting

effect mentioned previously diminished as the chordwise center of pressure approached the elastic axis with increase in normal-force coefficient. This effect is also seen in figure 8 for a Mach number of 0.80.

Effects of Sideslip

All of the preceding discussion has been concerned with flight conditions that produce symmetrical loading over the wings. However, in flight, an airplane frequently experiences sideslip motions either through actions of the pilot or owing to the dynamic response of the airplane. An extensive investigation at high subsonic speeds of this unsymmetrical loading condition has recently been made in the Langley high-speed 7- by 10-foot tunnel, and a few representative curves selected from these tests are presented in figures 10 and 11. These loads were measured on the 45° swept-wing—curved-body configuration shown in figure 2.

The data in figure 10 show for Mach numbers of 0.70 and 0.93 at an angle of attack of 4° that increase in sideslip angle β from 0° to 8° caused the load over the forward wing to increase, while the load over the rearward wing decreased by about the same amount. However, at an angle of attack of 8°, the load on the forward wing increased considerably over the reduction in load shown for the rearward wing.

Figure 11 shows the variation of the spanwise center of pressure with sideslip angle at Mach numbers of 0.70 and 0.93. These data show that variation of sideslip angle from 0° to 12° had no effect on the spanwise center of pressure for either the forward or the rearward wing. At the top of the figure is plotted the variations of the root bending-moment coefficient C_B with sideslip angle and from these curves it may be seen that although the spanwise center of pressure of the wings remained the same with increase in sideslip angle, the increase in load over the forward wing shown in figure 10 produced the increase in bending-moment coefficient shown in figure 11 for the forward wing.

CONCLUDING REMARKS

A study of the aerodynamic loads on sweptback wings at transonic speeds has indicated that for thick wings the spanwise center of pressure moves inward, whereas for thin wings, the spanwise center of pressure moves outboard with increase in Mach number. Also, increasing the sweep angle of a thin wing causes the spanwise center of pressure to move progressively outward. Then, washing out a thin swept wing shifted the spanwise center of pressure inboard and at a Mach number of 1.00, this inboard shift was primarily due to the loss in load over the trailing edges of the outboard portions of the span. Finally, an investigation of the effects of sideslip on the loads over a swept-wing—curved-body

combination has shown that increase in sideslip angle increased the relative load over the forward wing such that even though the spanwise center of pressure of the wings remained constant, the root bending-moment coefficients were increased.

Langley Aeronautical Laboratory,
National Advisory Committee for Aeronautics,
Langley Field, Va., May 4, 1953.

REFERENCES

1. Tinling, Bruce E., and Lopez, Armando E.: The Effects of Reynolds Number at Mach Numbers up to 0.94 on the Loading on a 35° Swept-Back Wing Having NACA 65_1A012 Streamwise Sections. NACA RM A52B20, 1952.

2. Loving, Donald L., and Williams, Claude V.: Aerodynamic Loading Characteristics of a Wing-Fuselage Combination Having a Wing of 45° Sweepback Measured in the Langley 8-Foot Transonic Tunnel. NACA RM L52B27, 1952.

3. Solomom, William, and Schmeer, James W.: Effect of Longitudinal Wing Position on the Pressure Characteristics at Transonic Speeds of a 45° Sweptback Wing-Fuselage Model. NACA RM L52K05a, 1953.

4. Rolls, L. Stewart, and Matteson, Frederick H.: Wing Load Distribution on a Swept-Wing Airplane in Flight at Mach Numbers up to 1.11, and Comparison With Theory. NACA RM A52A31, 1952.

[redacted]

EFFECTS OF THICKNESS ON CENTER-OF-PRESSURE LOCATION

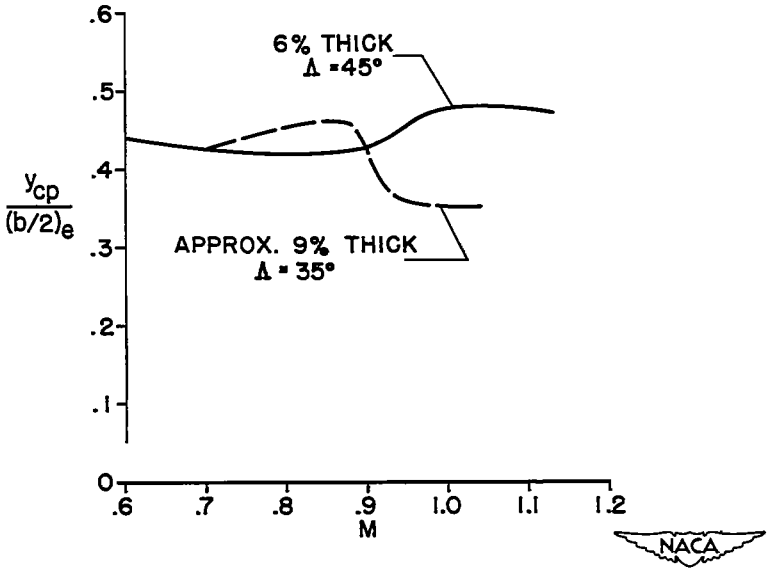

Figure 1.

VARIATION OF SPANWISE CENTER OF PRESSURE

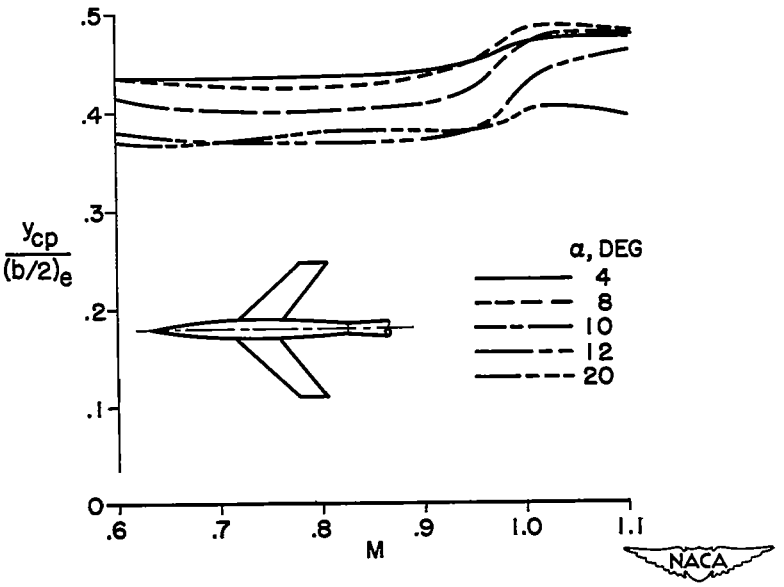

Figure 2.

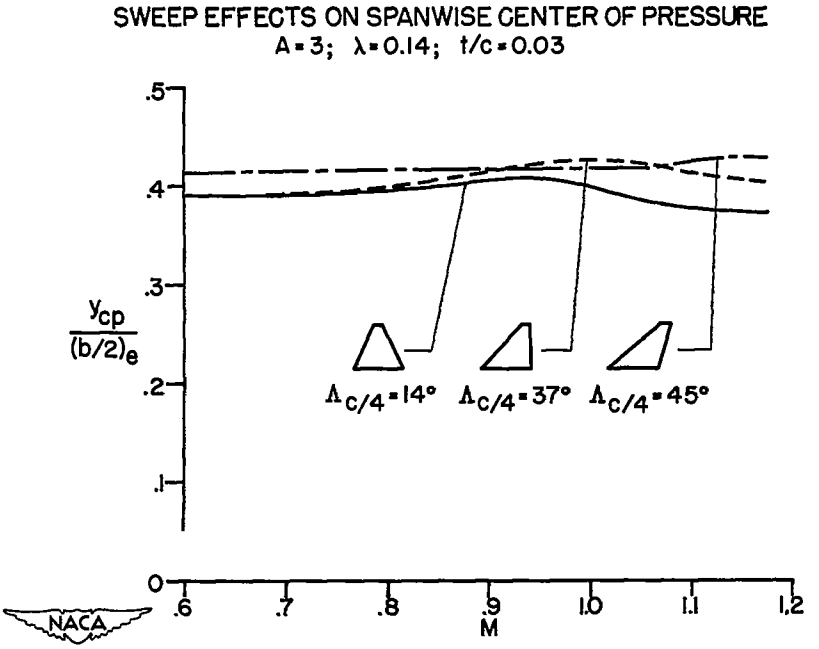

Figure 3.

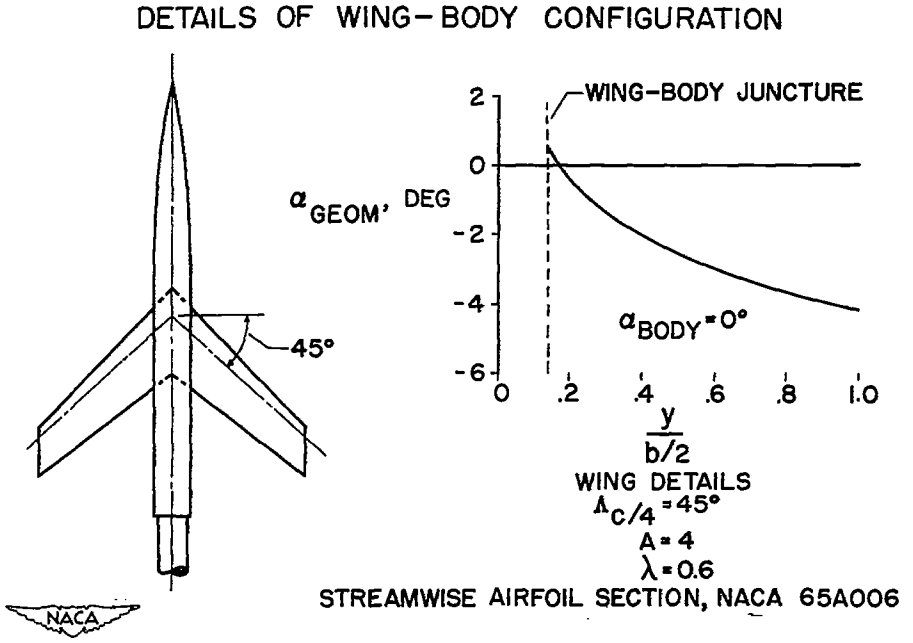

Figure 4.

WING SPANWISE LOAD DISTRIBUTION

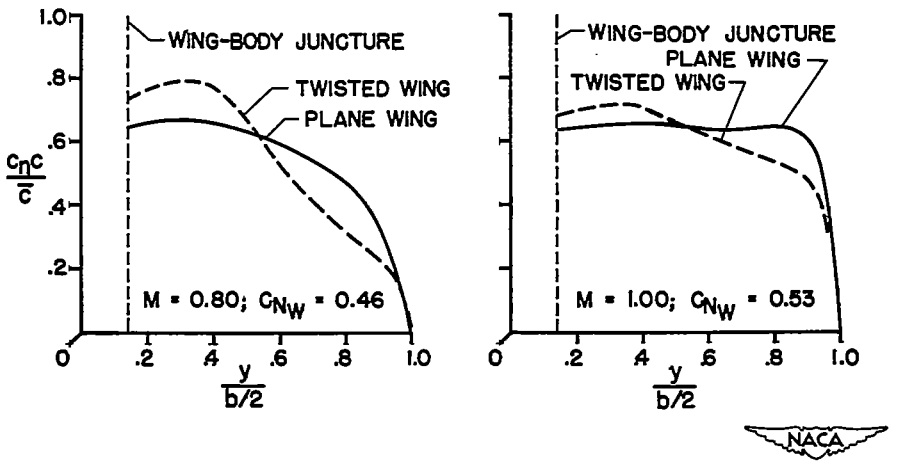

Figure 5.

COMPARISON OF PRESSURE-COEFFICIENT DISTRIBUTIONS

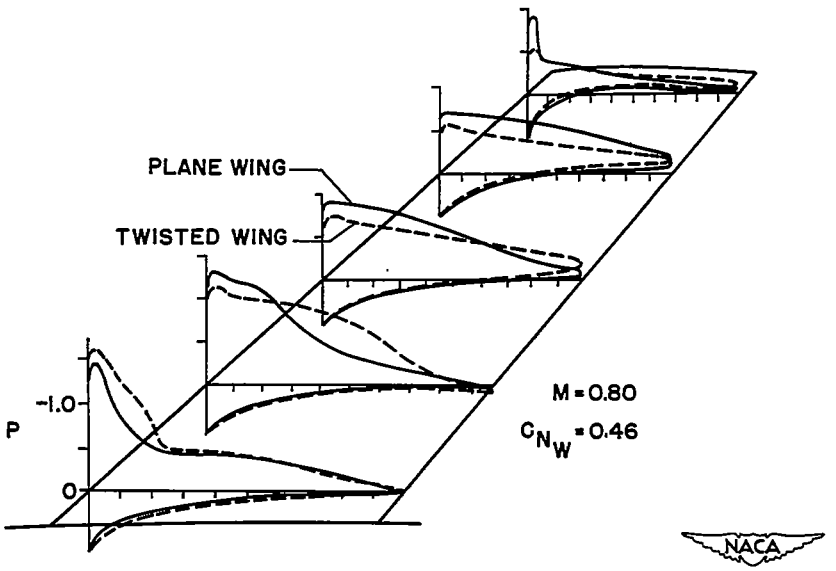

Figure 6.

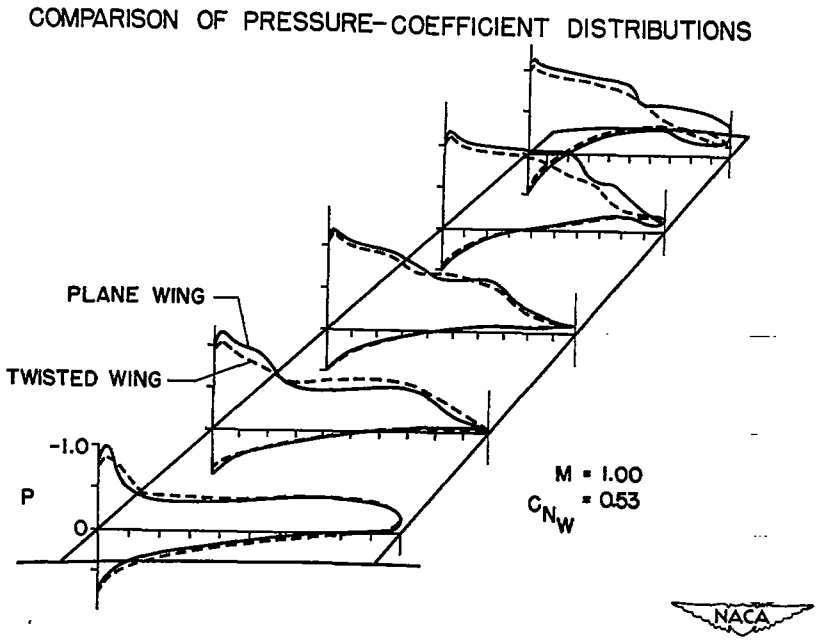

Figure 7.

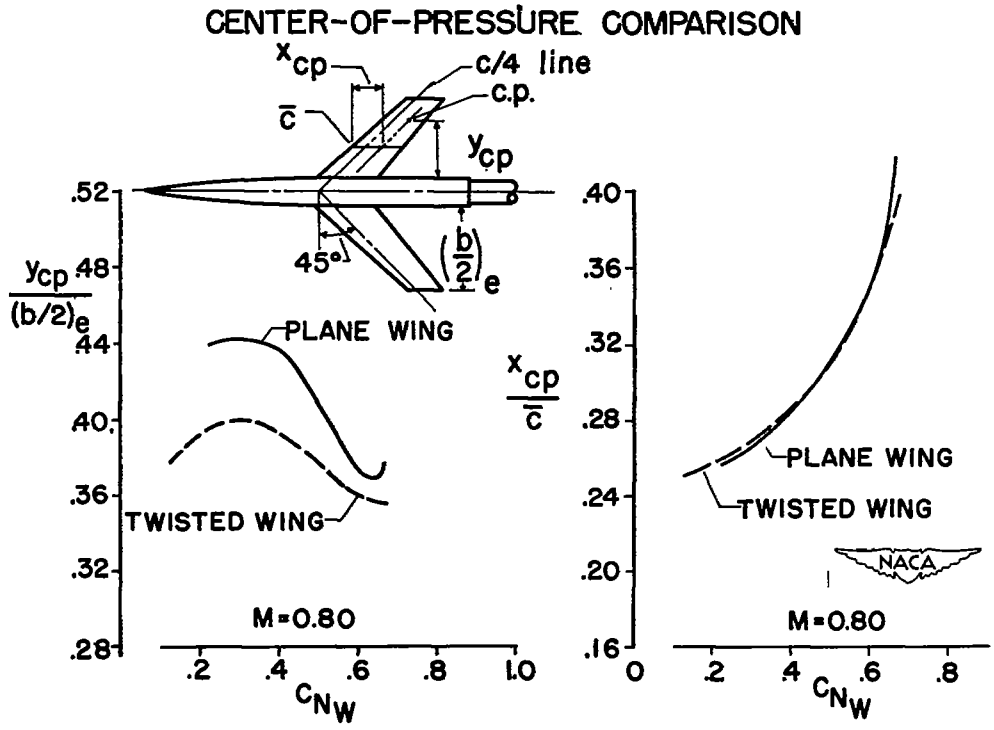

Figure 8.

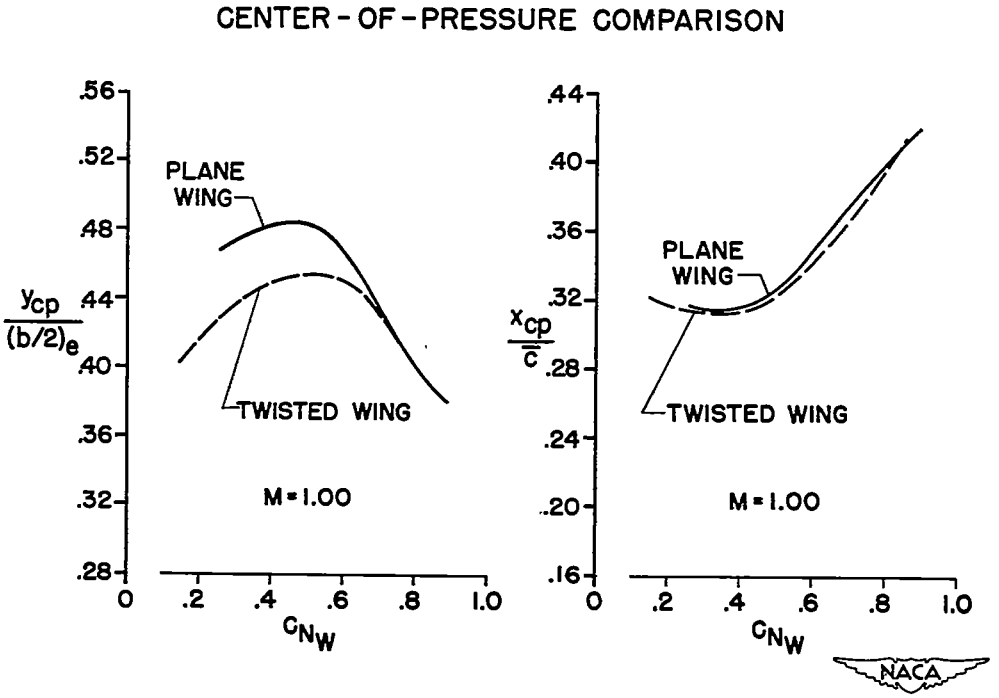

Figure 9.

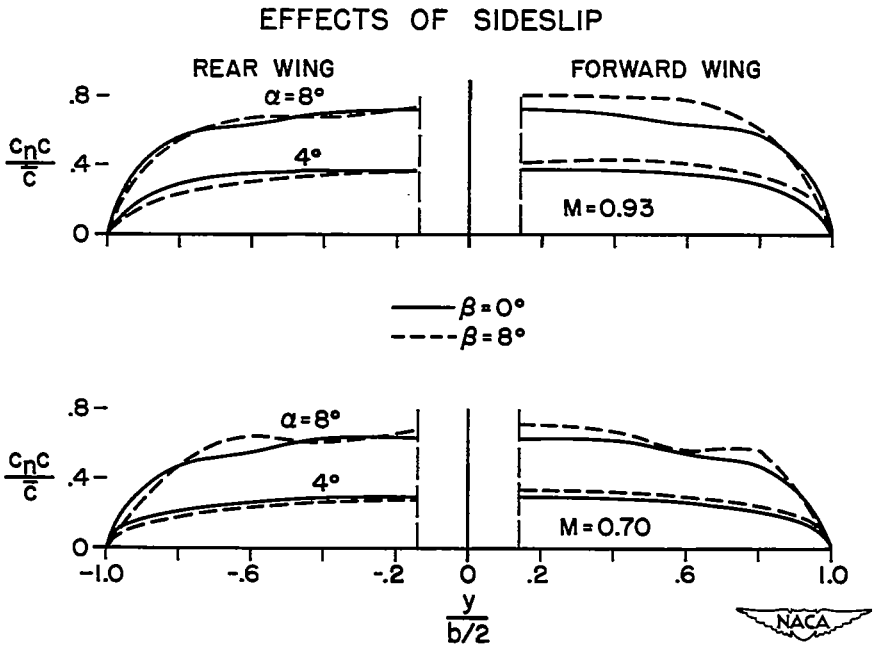

Figure 10.

[redacted]

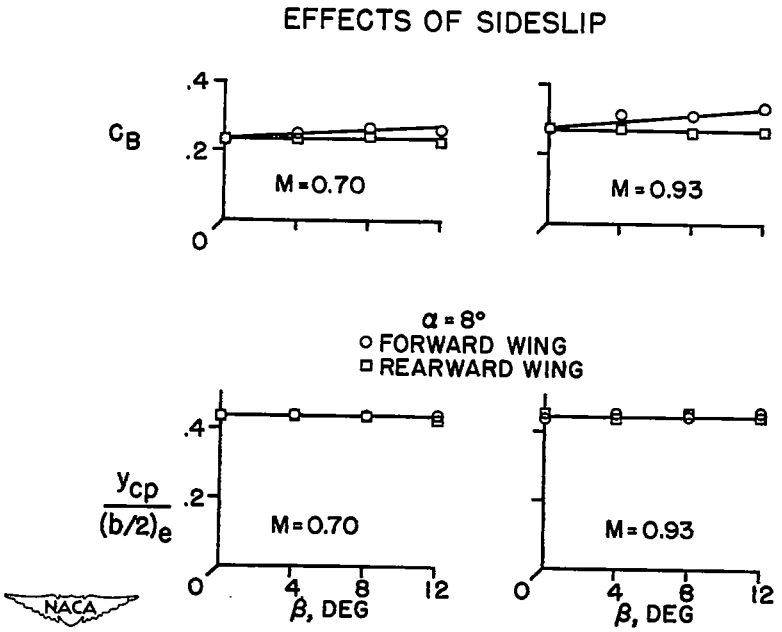

Figure 11.

NACA-Langley - 6-25-53 - 400